Stem Cell Reports
Article
ISSCR
OPEN ACCESS

In vitro differentiation of mouse pluripotent stem cells into corticosteroid-producing adrenocortical cells

Ioannis Oikonomakos,[1,2] Melina Tedesco,[1] Fariba Jian Motamedi,[1] Mirko Peitzsch,[3] Serge Nef,[4] Stefan R. Bornstein,[2] Andreas Schedl,[1,5,*] Charlotte Steenblock,[2,*] and Yasmine Neirijnck[1]
[1]Université Côte d'Azur, Inserm, CNRS, Institut de Biologie Valrose, 06108 Nice, France
[2]Department of Internal Medicine III, University Hospital Carl Gustav Carus, Technische Universität Dresden, Dresden, Germany
[3]Institute of Clinical Chemistry and Laboratory Medicine, University Hospital Carl Gustav Carus, Medical Faculty Carl Gustav Carus, Technische Universität Dresden, Dresden, Germany
[4]Department of Genetic Medicine and Development, University of Geneva, 1211 Geneva, Switzerland
[5]Lead contact
*Correspondence: schedl@unice.fr (A.S.), charlotte.steenblock@ukdd.de (C.S.)
https://doi.org/10.1016/j.stemcr.2024.07.010

SUMMARY

Directed differentiation of pluripotent stem cells into specialized cell types represents an invaluable tool for a wide range of applications. Here, we have exploited single-cell transcriptomic data to develop a stepwise *in vitro* differentiation system from mouse embryonic stem cells into adrenocortical cells. We show that during development, the adrenal primordium is embedded in an extracellular matrix containing tenascin and fibronectin. Culturing cells on fibronectin during differentiation increased the expression of the steroidogenic marker NR5A1. Furthermore, 3D cultures in the presence of protein kinase A (PKA)-pathway activators led to the formation of aggregates composed of different cell types expressing adrenal progenitor or steroidogenic markers, including the adrenocortical-specific enzyme CYP21A1. Importantly, *in-vitro*-differentiated cells responded to adrenocorticotropic hormone (ACTH) and angiotensin II with the production of glucocorticoids and mineralocorticoids, respectively, thus confirming the specificity of differentiation toward the adrenal lineage.

INTRODUCTION

The adrenal cortex is a vital component of the body's regulatory system regulating blood pressure, metabolism, and the response to stress and infections through the release of steroid hormones. Steroids are produced in highly specialized zones that are arranged in concentric rings including the mineralocorticoid-producing zona glomerulosa (zG), the glucocorticoid-producing zona fasciculata (zF), and the androgen-producing zona reticularis (zR). Mouse adrenals lack a functional zR but have a juxtamedullary X-zone, a remnant of the fetal cortex that disappears in males at puberty and in females after the first pregnancy (Walczak and Hammer, 2015). Given the important function of adrenals, it is not surprising that adrenal insufficiencies, such as Addison's disease and congenital adrenal hyperplasia, can be life-threatening if left untreated (Hellesen et al., 2018; Speiser et al., 2010). Hormone therapy is the primary treatment, but maintaining adequate hormone levels can be challenging, leading to hormonal fluctuations that can affect the quality of life and increase the risk of adrenal crisis (Lightman et al., 2020).

A potential cure for adrenal insufficiency may be the transplantation of functional adrenocortical cells capable of responding to adrenocorticotropic hormone (ACTH) to ensure an adequate release of glucocorticoids. Functional steroidogenic cells have previously been generated by forced expression of the transcription factor NR5A1 (Crawford et al., 1997; Ruiz-Babot et al., 2018; Sonoyama et al., 2012), a master regulator of steroidogenesis (Parker and Schimmer, 1997). However, overexpression of NR5A1 results in abnormal steroid hormone production, thus limiting the use of such a system for therapeutic approaches. The development of protocols that allow directed differentiation of pluripotent stem cells into adrenocortical cells could potentially overcome this problem. In a recent study, human induced pluripotent stem cells (hiPSCs) were used to generate steroidogenic cells, but instead of glucocorticoids, these cells produced dehydroepiandrosterone (DHEA), a precursor of androgens and estrogens (Sakata et al., 2022). *In vitro* differentiation of pluripotent stem cells into glucocorticoid-producing cells has not yet been reported.

To develop an *in vitro* differentiation protocol, a detailed knowledge of adrenal development is essential. Adrenocortical progenitors are mesoderm-derived and emerge from the adrenogonadal primordium (AGP), a structure traditionally defined by *Nr5a1* expression and located at the interface of the intermediate mesoderm (IM) and the lateral plate mesoderm (LPM) (Ikeda et al., 1994). Recent advances using single-cell transcriptomic analysis in mice (Neirijnck et al., 2023; Sasaki et al., 2021) and humans (Cheng et al., 2022) have permitted further insights into the adrenal origin. In particular, these studies have revealed that adrenocortical cell fate is specified prior to *Nr5a1* expression, at the anterior end of the developing urogenital ridge.

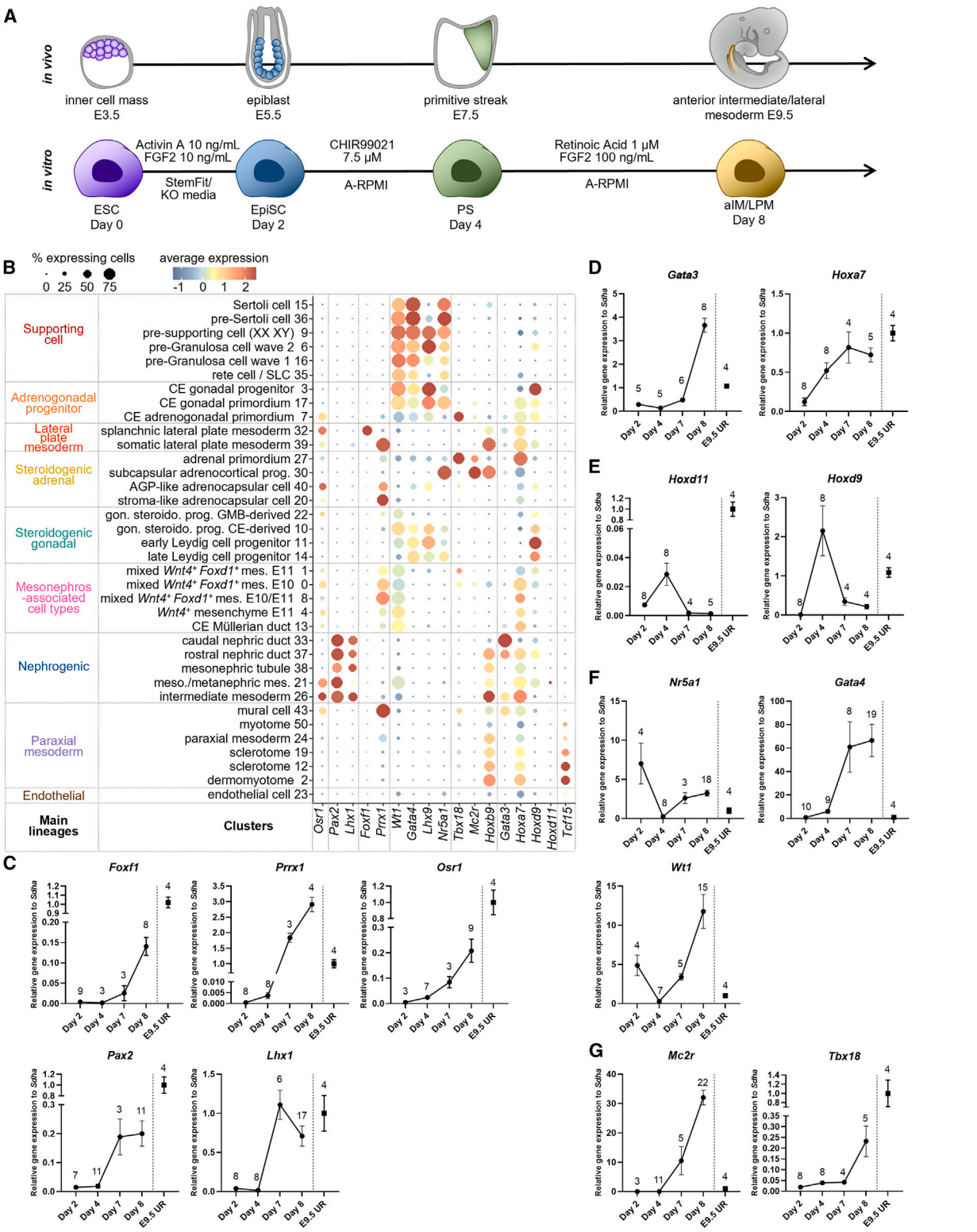

(legend on next page)

Here, we have leveraged these findings to develop a stepwise differentiation protocol of mouse pluripotent embryonic stem cells (mESCs) into adrenocortical cells via anterior intermediate/lateral plate mesodermal progenitors. Importantly, when cultured in 3D, the aggregates endogenously express key markers of adrenocortical cells and secrete the steroids corticosterone/11-dehydrocorticosterone and aldosterone, when treated with ACTH and angiotensin II, respectively.

RESULTS

Directed differentiation of mESCs into anterior intermediate/lateral mesoderm induces expression of early adrenocortical progenitor markers

Early mammalian development involves the differentiation of embryonic stem cells (ESCs) into epiblast stem cells (EpiSCs), transitioning from naive to primed pluripotency. Epiblastic cells further undergo an epithelial-to-mesenchymal transition to give rise to the primitive streak (PS), a transient embryonic structure comprising mesendodermal precursors that can be induced by canonical Wnt signaling both *in vivo* and *in vitro* (Schnirman et al., 2023) (Figure 1A). To convert mESCs into EpiSCs, we first treated mESCs with activin and fibroblast growth factor 2 (FGF2) for 2 days, as previously described (Tosolini and Jouneau, 2016), resulting in upregulation of the EpiSC marker *Fgf5* (Figures S1A and S1B). We next induced Wnt/β-catenin signaling with the GSK3-α/β inhibitor Chiron (CHIR99021) for 2 days (Lam et al., 2014; Takasato et al., 2015) and observed induction of the PS as evidenced by robust upregulation of *Brachyury* (*T*) at day 4 of differentiation (Figure S1B).

Previous work has shown that hiPSC-derived PS cells spontaneously differentiate into definitive endoderm and mesodermal subtypes, a cell fate that can be redirected toward IM by the exogenous addition of FGF2 (Lam et al., 2014) and anteriorized by the addition of retinoic acid (RA) (Takasato et al., 2015). We tested whether treatment of mESC-derived PS cells with these factors would direct specification toward the anterior IM and/or LPM, which would provide adequate conditions for the specification into adrenocortical progenitors. To allow fine-tuning of differentiation protocols, we first analyzed our recently published single-cell transcriptomic atlas (Neirijnck et al., 2023) to establish a set of suitable developmental markers that highlight specific lineages and stages (Figure 1B). Consistent with earlier reports (Mugford et al., 2008), *Osr1* was found to be expressed at early stages in IM (cluster [C] 26), nephrogenic mesenchyme (C21), mesonephros-associated cell types (C1, C0, C8, C4, and C13), and LPM (C32 and C39), but was absent in paraxial mesoderm (C2, C12, C19, and C24). We therefore considered this gene as a marker for both IM and LPM. In contrast, expression of *Pax2/Lhx1* (Kobayashi et al., 2005; Plachov et al., 1990) and *Foxf1/Prrx1* (Mahlapuu et al., 2001; Sefton et al., 2018) is mutually exclusive in the IM and LPM lineages, respectively, confirming previous reports. Early adrenogonadal progenitors (C7) expressed the transcription factors *Wt1*, *Gata4*, *Lhx9*, and *Tbx18* and low levels of *Nr5a1*. As the cells progressed through the adrenal (C27 and C30) or gonadal (C17 and C3) lineages, they exhibited distinct transcriptional profiles with expression of *Tbx18/Mc2r/Hoxb9* and *Wt1/Gata4/Lhx9*, respectively, while *Nr5a1* was upregulated in both lineages. In addition, the expression of the anterior *Hoxa7* and posterior *Hoxd9* genes distinguishes the adrenal primordium (C27) from the gonadal primordium (C17), respectively, reflecting lineage specification along the anteroposterior axis (Neirijnck et al., 2023). Treatment of mESC-derived PS cells with FGF2 and RA for 4 days (day 8 of the differentiation protocol) resulted

Figure 1. Differentiation of mESCs into anterior intermediate/lateral mesoderm is associated with early adrenocortical marker expression

(A) Schematic overview of anterior intermediate/lateral mesoderm formation *in vivo* (top panel) and stepwise mESC differentiation *in vitro* (bottom panel). Cells were treated for 2 days with Activin A and FGF2, followed by two days with CHIR99021 and then 4 days with retinoic acid and FGF2 (see also experimental procedures). aIM/LPM, anterior intermediate/lateral plate mesoderm; E, embryonic day; EpiSC, epiblast stem cell, ESC, pluripotent embryonic stem cell; PS, primitive streak.

(B) Dot plot showing expression of selected marker genes (x axis) per cluster (y axis) of the mesodermal-derived cell lineages from (Neirijnck et al., 2023). The size of the dot represents the percentage of cells in the cluster expressing the gene, and the color indicates the level of expression (log normalized counts). Cluster annotation and major cell lineages are displayed on the left. AGP, adrenogonadal primordium; CE, coelomic epithelium; E, embryonic day; GMB, gonad/mesonephros border; gon. steroido. prog., gonadal steroidogenic progenitor; mes., mesenchyme; meson., mesonephric; SLC, supporting-like cell.

(C–G) RT-qPCR for marker genes of intermediate and lateral plate mesoderm (*Foxf1-Pax2***; *Prrx1-Osr1****; *Lhx1*****) (C), antero-posterior patterning of the urogenital ridge (*Hoxd9-Hoxd11-Hoxa7***; *Gata3*****) (D and E), early adrenogonadal progenitors (*Gata4***; *Wt1****; *Nr5a1*****) (F), and early adrenocortical progenitors (*Tbx18***; *Mc2r*****) (G), during the progress of *in vitro* differentiation. Data depict relative mRNA expression levels, presented as mean ± SEM values of biological replicates (number indicated on the graphs) and normalized to E9.5 mouse urogenital region (E9.5 UR, pools of 4–6 embryos). Welch's ANOVA test was performed resulting in significant difference among means. ** = $p < 0.01$; *** = $p < 0.001$; **** = $p < 0.0001$. See also Figure S1.

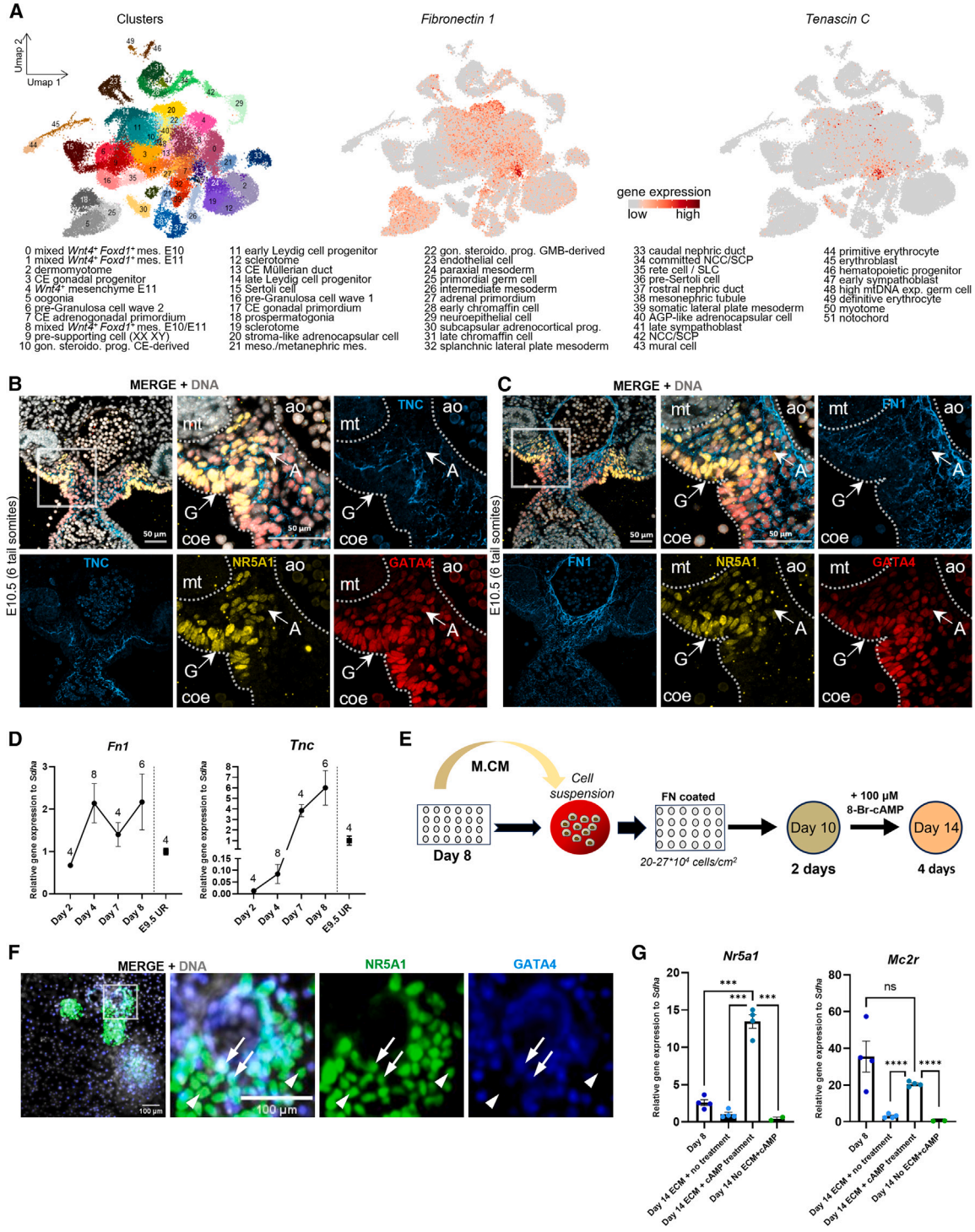

Figure 2. Adrenocortical progenitors differentiate in a fibronectin/tenascin C-rich environment

(A) Uniform manifold approximation and projection (UMAP) visualization of the 72,273 transcriptomes from (Neirijnck et al., 2023) colored by clusters and by expression levels of *fibronectin 1* (*Fn1*) and *tenascin C* (*Tnc*). Cluster annotation is shown on the bottom. AGP, adrenogonadal primordium; CE, coelomic epithelium; GMB, gonad/mesonephros border; gon. steroido. prog., gonadal steroidogenic progenitor; mes., mesenchyme; meson., mesonephric; mtDNA exp., mitochondrial DNA expressing; NCC, neural crest cell; SLC, supporting-like cell; SCP, Schwann cell precursor.

(legend continued on next page)

in strong expression of *Foxf1*, *Prrx1*, *Osr1*, *Pax2*, and *Lhx1* (Figure 1C), indicating differentiation into IM and LPM cells. Paraxial mesoderm (*Tcf15*) and endoderm (*Pdx1*) markers were not upregulated (Figure S1C), thus confirming the specificity of the differentiation. Further analysis revealed higher expression levels of anterior (*Gata3/Hoxa7*) than posterior (*Hoxd9/Hoxd11*) markers (Figures 1D and 1E) (Takasato et al., 2015), suggesting that the cells were adopting an anterior intermediate/LPM (aIM/LPM) fate. Interestingly, this was concomitant with the induction of the adrenogonadal progenitor markers *Wt1*, *Gata4*, and *Nr5a1* (Figure 1F) and an increase in the adrenocortical progenitor marker genes *Tbx18*, *Hoxb9*, and *Mc2r*, encoding the ACTH receptor (Figures 1G and S1D). By contrast, the gonadal-enriched gene *Lhx9* was not found to be induced, suggesting differentiation toward the adrenal rather than the gonadal lineage (Figure S1D). The steroidogenic marker *Nr5a1*, which is expressed at low levels in ESCs (Clipsham et al., 2004) but is lost during differentiation to the PS state, showed only a mild induction upon FGF2 and RA treatment, in contrast to *Wt1*, whose expression kept increasing over time (Figure S1E). To confirm the reproducibility of our differentiation protocol, we established an XX ESC line from blastocysts isolated from the *Nr5a1*-eGFP^{Tg} reporter mouse line (Stallings et al., 2002), contrasting the XY R1 cell line used for the initial protocol development. Quantitative reverse-transcription PCR (RT-qPCR) analysis at day 8 of the differentiation protocol revealed comparable levels of *Osr1*, *Nr5a1*, *Mc2r*, and *Gata3* expression between the two cell lines (Figure S1F).

Extracellular matrix promotes endogenous NR5A1 expression

We (Neirijnck et al., 2023) and others (Häfner et al., 2015) have previously shown that early adrenocortical cells are specified prior to *Nr5a1* expression. The expression of the adrenocortical-enriched genes *Tbx18*, *Hoxa7*, *Hoxb9*, and *Mc2r* at day 8 of differentiation, but the absence of high levels of *Nr5a1*, suggested that the cells had committed toward the adrenocortical lineage but had failed to fully differentiate. To drive the aIM/LPM cells toward the steroidogenic fate, we aimed to mimic the *in vivo* adrenocortical environment with a focus on extracellular matrix (ECM) proteins. Analysis of our single-cell atlas revealed that adrenogonadal progenitors specifically express *tenascin C* (*Tnc*), while several cell types express *fibronectin 1* (*Fn1*) (Figure 2A). Immunostaining confirmed TNC expression in NR5A1$^+$ cells at embryonic day (E) 10.5 (Figure 2B), whereas FN1 was more widely expressed (Figure 2C). Interestingly, *Tnc* expression was strongly induced (~100-fold) from day 4 to day 8 in our *in vitro* system, further supporting the correct fate of the cells toward the adrenogonadal lineage. *Fn1* expression remained stable during this period (Figure 2D).

We next aimed to replicate the FN1-rich environment in our *in vitro* system. Day 8 cells were detached from their original collagen- and laminin-based ECM (Geltrex) and replated onto plates coated with FN1. To wean the cells from their familiar environment, day 8 mesodermal conditioned media (M.CM) were added during the introduction of the new ECM (Caneparo et al., 2020). *Nr5a1* expression has been shown to be stimulated by protein kinase A (PKA) signaling (Drelon et al., 2016; Kulcenty et al., 2015). We therefore added 8-Br-cAMP (a stable analog of cAMP) after two days in the new culture conditions (Figure 2E). After a further 4 days of differentiation, the colonies contained cells with strong NR5A1 expression surrounded by GATA4$^+$ cells (Figure 2F). RT-qPCR analysis confirmed that the combination of FN1 coating and cAMP supplementation resulted in a strong increase in *Nr5a1* expression compared to FN1 coating or cAMP supplementation alone

(B) Co-labeling for GATA4, NR5A1, and TNC (immunostaining) in E10.5 embryos (transverse sections), revealing TNC expression in mesenchymal cells underlying the coelomic epithelium, including the adrenal primordium. Nuclei are stained with Hoechst. A, adrenal field; ao, aorta; coe, coelomic cavity; G, gonadal field; mt, mesonephric tubule. Scale bars, 50 μm.

(C) Co-labeling for GATA4, NR5A1, and FN1 (immunostaining) in E10.5 embryos (transverse sections), revealing broad FN1 expression in mesenchymal cells. Nuclei are stained with Hoechst. A, adrenal field; ao, aorta; coe, coelomic cavity; G, gonadal field; mt, mesonephric tubule. Scale bars, 50 μm.

(D) RT-qPCR for *Fn1* (*) and *Tnc* (**) during the progress of *in vitro* differentiation. Data depict relative mRNA expression, presented as mean ± SEM values of biological replicates (number indicated on the graphs) and normalized on E9.5 mouse urogenital region (E9.5 UR, pools of 4–6 embryos). Welch's ANOVA test was performed resulting in significant difference among means. * = $p < 0.05$; ** = $p < 0.01$.

(E) Schematic overview of aIM/LPM cells (day 8) differentiation on FN-coated plates. Cells were treated for 2 days with M.CM and for 2 days with 8-Br-cAMP (see also experimental procedures).

(F) Co-labeling for NR5A1 and GATA4 in day 14 differentiated cells, revealing NR5A1$^+$ colonies. Nuclei are stained with Hoechst. Scale bars, 100 μm. Arrows indicate NR5A1$^+$/GATA4$^+$ cells and arrowheads indicate NR5A1$^+$/GATA4$^-$ cells.

(G) RT-qPCR for *Nr5a1* and *Mc2r* on aIM/LPM cells (day 8, dark blue) and on day 14 cells cultured on FN1 (ECM treatment) alone (light blue) or with 8-Br-cAMP supplementation (turquoise), and with 8-Br-cAMP supplementation alone (green) (see also experimental procedures). Data depict relative mRNA expression, presented as mean ± SEM values of biological replicates (n = 2 to 4) and normalized to E9.5 mouse urogenital region (pools of 4–6 embryos, n = 4). Statistical analysis was performed using two-tailed unpaired Welch's t test. ns., not significant; *** = $p < 0.001$; **** = $p < 0.0001$.

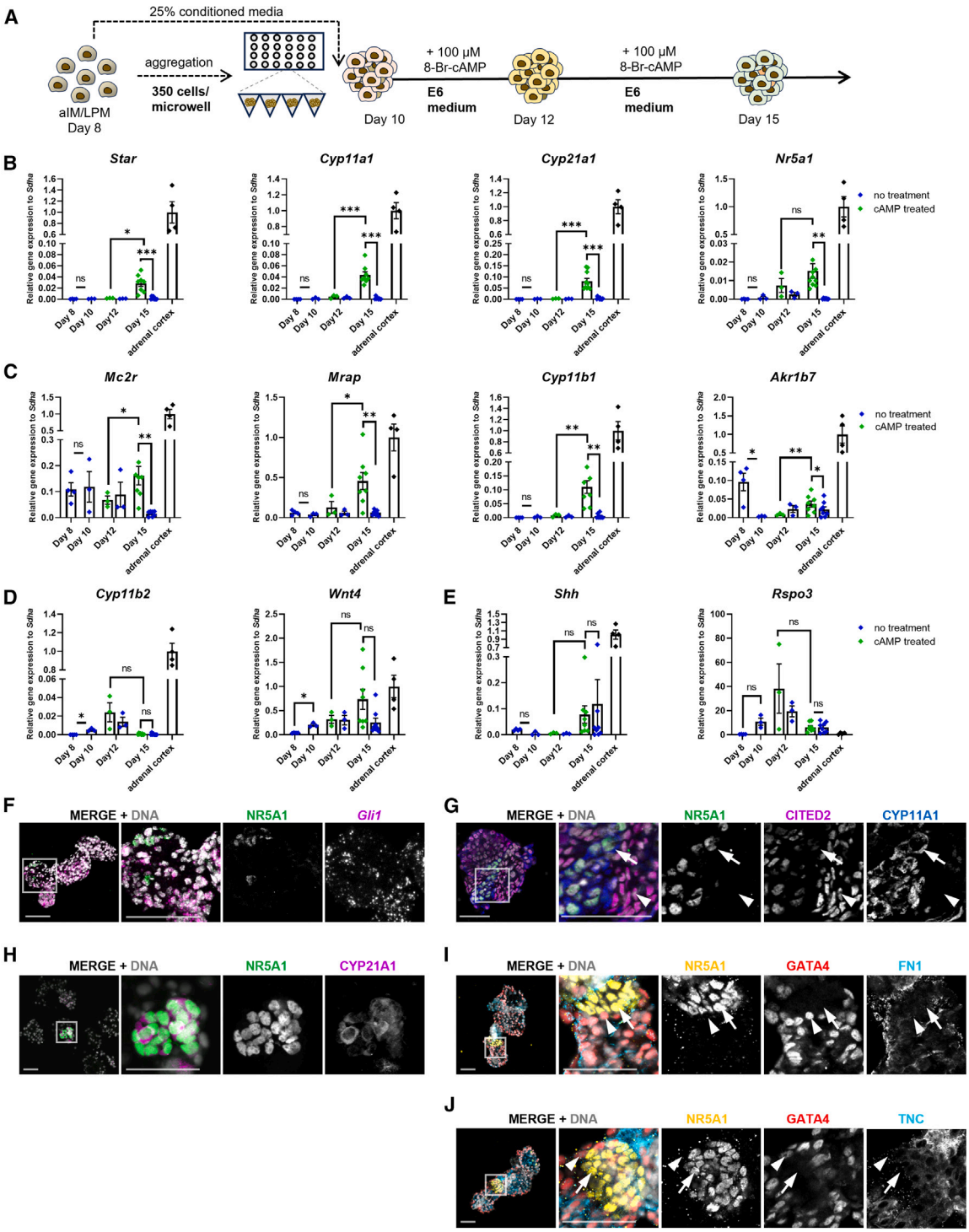

Figure 3. Differentiation of aIM/LPM cells with 3D assembly leads to a steroidogenic fate

(A) Schematic overview of aIM/LPM cell differentiation. Cells are aggregated on microwell plates and treated for 2 days with M.CM and 5 days with 8-Br-cAMP (see also experimental procedures).

(B–E) RT-qPCR analysis for the steroidogenic genes *Star*, *Cyp11a1*, *Cyp21a1*, and *Nr5a1* (B), the corticosterone production-related genes *Mc2r*, *Mrap*, *Cyp11b1*, and the zona fasciculata marker *Akr1b7* (C), the aldosterone production-related genes *Cyp11b2* and *Wnt4* (D), and the adrenocortical progenitor markers *Rspo3* and *Shh* (E), during the progress of *in vitro* differentiation. Data depict relative mRNA expression,

(legend continued on next page)

(Figure 2G). Expression of *Mc2r* was maintained under FN1/cAMP conditions but decreased in the presence of FN1 or cAMP alone.

3D cultures of *in-vitro*-derived aIM/LPM cells induce adrenocortical-specific steroidogenic gene expression

In other systems, 3D cultures have been shown to be more conducive to differentiation by providing molecular cues from neighboring cells as well as mechanical stimulation (Dedhia et al., 2023; Kapałczyńska et al., 2018). We therefore tested the aggregation of aIM/LPM cells in ultra-low attachment plates, or in microwell plates, the latter allowing the formation of hundreds of small spheroids in a single well. After 2 days in M.CM (day 10 of differentiation), aggregates were treated with or without 8-Br-cAMP for 5 days (day 15 of differentiation) (Figure 3A). RT-qPCR analysis at days 8, 10, 12, and 15 was performed to evaluate the expression dynamics of adrenocortical-specific markers. Culturing in microwell plates generally resulted in higher activation of steroidogenic genes than in ultra-low attachment plates (Figures S2A and S2B) and this method was chosen for all further experiments.

cAMP stimulation led to a significant increase in *Nr5a1*, the cholesterol transporter *Star*, the steroidogenic enzyme *Cyp11a1*, and the adrenal-specific enzyme *Cyp21a1*, although the levels remained lower than in adrenal cortex microdissected from adult mice (Figure 3B). Medium without 8-Br-cAMP supplementation resulted in significantly lower expression of these genes. Analysis of markers specific for glucocorticoid-producing zF cells revealed cAMP-dependent induction of *Cyp11b1* and *Mc2r-accessory protein* (*Mrap*), and cAMP-dependent maintenance of *Mc2r* expression (Figure 3C), which appeared to be in a dose-dependent manner (Figure S2C). *Akr1b7* was expressed at day 15 independently of the treatment (Figure 3C). Similar results were obtained with the *Nr5a1-eGFP* cell line (Figure S2D). Moreover, fluorescent imaging of this cell line revealed activation of the *Nr5a1* promoter-driven GFP from day 12 onward (Figure S2E).

Markers of mineralocorticoid-producing zG cells, *Cyp11b2*, *Wnt4*, and *Dab2* were also induced during differentiation, but this was independent of cAMP treatment (Figures 3D and S3A). Moreover, the expression of the key gene for mineralocorticoid production (*Cyp11b2*) was far lower than *in vivo*. Interestingly, *Rspo3* and *Shh*, which are expressed in capsular or subcapsular progenitors of the definitive adult cortex (King et al., 2009; Vidal et al., 2016), remained highly expressed with and without cAMP stimulation (Figure 3E). This suggests that both differentiated steroidogenic and progenitor cell populations persist under these culture conditions. Importantly, no significant levels of the gonadal progenitor marker *Lhx9*, the supporting cell markers *Wt1*, *Sox9*, and *Foxl2* (Stévant et al., 2019), nor of the testicular steroidogenic enzyme *Hsd17b3* (Labrie et al., 2000) were observed (Figures S3B–S3D), indicating specificity of differentiation toward the adrenal lineage.

To gain further insight into the architecture of the aggregates, we performed RNAscope *in situ* hybridization analysis for *Gli1*, a marker for the progenitor reservoir of the adrenal cortex during development and tissue maintenance (Wood et al., 2013). *Gli1* expression was found in a high proportion of cells consistent with the persistence of large numbers of progenitors (Figure 3F). Immunostaining for NR5A1, CYP11A1, CYP21A1, the adrenal primordium marker CITED2 (Val et al., 2007), and the adrenogonadal progenitor markers GATA4 and WT1 (Figures 3G, 3H, and S3E) revealed the presence of NR5A1$^+$/CYP21A1$^+$ and NR5A1$^+$/CYP11A1$^+$ cells, whereas the majority of CITED2$^+$, GATA4$^+$, and WT1$^+$ cells were negative for NR5A1, indicating that both differentiated and non-steroidogenic progenitor cells are present in the aggregates, in agreement with our qPCR analysis. Moreover, immunostaining for FN1 and TNC showed an enrichment of these ECM proteins in the aggregates (Figures 3I and 3J), indicating that 3D cultured cells produce ECM proteins that are also found *in vivo*.

Aggregates produce glucocorticoids

The expression of genes involved in the processing of steroidogenic enzymes and the presence of *Cyp11b1* suggested that the *in-vitro*-differentiated aggregates were able

presented as mean ± SEM values of biological replicates (day 8 $n = 4$, day 10 $n = 3$, day 12 treated and not treated $n = 3$, day 15 treated and not treated $n = 8$) (not treated: blue, cAMP treated: green), and normalized on adult adrenal cortex + capsule (black) ($n = 4$). Statistical analysis was performed using two-tailed unpaired Welch's t test. ns., not significant; * = $p < 0.05$; ** = $p < 0.01$; *** = $p < 0.001$.

(F) Co-labeling for NR5A1 (immunostaining) and *Gli1* mRNA (RNAScope *in situ* hybridization) on day 15 paraffin-embedded aggregates.

(G) Co-labeling for NR5A1, CITED2, and CYP11A1 on day 15 paraffin-embedded aggregates. Arrow indicates NR5A1$^+$/CYP11A1$^+$/CITED2$^-$ cell and arrowhead indicates NR5A1$^-$/CYP11A1$^-$/CITED2$^+$ cells.

(H) Co-labeling for NR5A1 and CYP21A1 on day 15 paraffin-embedded aggregates.

(I) Co-labeling for NR5A1, GATA4, and FN1 on day 15 paraffin-embedded aggregates. Arrow and arrowhead indicate NR5A1$^+$/GATA4$^-$ and NR5A1$^-$/GATA4$^+$ cells, respectively.

(J) Co-labeling for NR5A1, GATA4, and TNC on day 15 paraffin-embedded aggregates. Arrow and arrowhead indicate NR5A1$^+$/GATA4$^-$ and NR5A1$^-$/GATA4$^+$ cells, respectively. Nuclei are stained with DAPI or Hoechst. Scale bars, 50 μm. See also Figures S2 and S3.

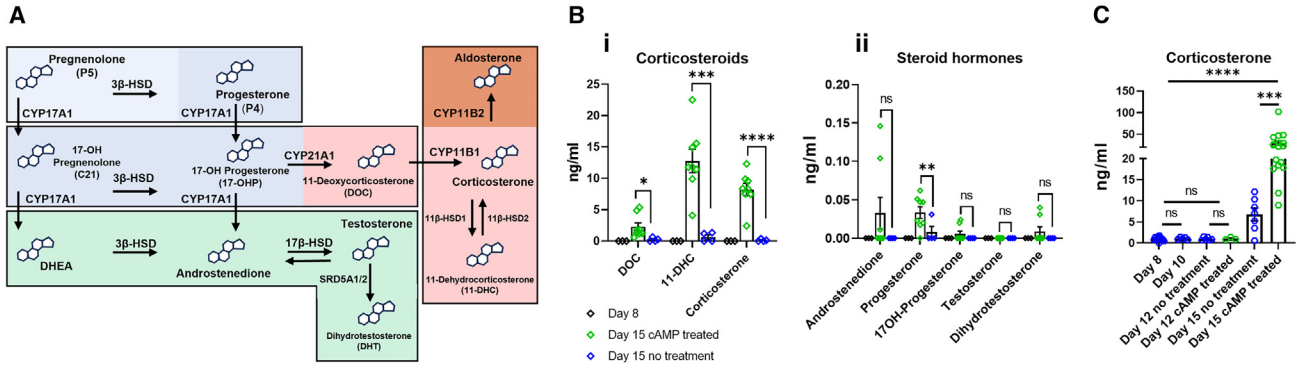

Figure 4. *In-vitro*-differentiated aggregates produce glucocorticoids

(A) Illustration of the steroid production pathway in mice, delineating the key genes responsible for synthesizing progestogens (blue box), corticosteroids (red box), and androgens (green box).

(B) LC-MS/MS analysis for corticosteroids (i) and progestogens/androgens (ii) on M.CM (day 8) and aggregates medium (day 15) treated or not with 8-Br-cAMP. Data depict steroid concentrations as ng/mL of medium, presented as mean ± SEM values of biological replicates (day 8 [black] $n = 3$, day 15 cAMP treated [green] $n = 8$, day 15 not treated [blue] $n = 4$). Statistical analysis was performed using two-tailed unpaired Welch's t test. ns, not significant; * = $p < 0.05$; ** = $p < 0.01$; *** = $p < 0.001$; **** = $p < 0.0001$. DOC, 11-deoxycorticosterone; 11-DHC, 11-dehydrocorticosterone. See also Table S1.

(C) ELISA measurement of corticosterone levels in M.CM (day 8) and medium collected from aggregate cultures (days 10, 12, and 15) treated (green) or not (blue) with 8-Br-cAMP. Data depict corticosterone concentrations as ng/mL of medium, presented as means ± SEM values of biological replicates (day 8 $n = 11$, day 10 $n = 5$, day 12 cAMP treated $n = 3$, day 12 not treated $n = 6$, day 15 cAMP treated $n = 17$, day 15 not treated $n = 7$). Statistical analysis was performed using two-tailed unpaired Welch's t test. ns, not significant; *** = $p < 0.001$; **** = $p < 0.0001$.

to produce zF-specific steroids (Figure 4A). To address this possibility, we collected medium on day 15 and performed steroid hormone analysis by liquid chromatography with tandem mass spectrometry (LC-MS/MS) (Peitzsch et al., 2015). The 8-Br-cAMP-treated samples showed the presence of the main mouse glucocorticoids corticosterone (~8 ng/mL), 11-dehydrocorticosterone (~12 ng/mL), and 11-deoxycorticosterone (~2 ng/mL) in the media (Figure 4B). No mineralocorticoids (aldosterone) were detected (Table S1). Importantly, sex steroids such as testosterone and dihydrotestosterone were barely detectable (Figure 4B), indicating a high specificity of adrenocortical steroid production in the *in-vitro*-differentiated aggregates. Furthermore, ELISA analysis indicated that the initiation of corticosterone production occurred after day 12 of differentiation (Figure 4C), a finding that is consistent with the late induction of steroidogenic genes (Figures 3B and 3C).

Aggregates respond to physiological stimuli *in vitro*

Adrenocortical cells respond to the physiological signals ACTH and angiotensin II by producing glucocorticoids and mineralocorticoids, respectively. To test whether aggregates also respond to these stimuli, we first treated day 12 cultures with Synacthen, a synthetic ACTH analog that is used in medical practice (Figure 5A). Synacthen-treated cells showed increased expression of *Cyp11b1* (Figure 5Bi), but no change for *Cyp21a1*, *Mrap*, and *Nr5a1* expression (Figure S4A), which is consistent with the results obtained for cAMP-treated samples. Importantly, Synacthen treatment also boosted corticosterone production as measured by mass spectrometry (Figure 5Bii).

Aldosterone production requires the expression of *Cyp11b2*, and we have already observed a low expression level of this gene at day 12 of our culture system, which however had disappeared by day 15 (Figure 3D). Angiotensin II treatment of day 12 cultures resulted in a significant increase of *Nr5a1* and *Cyp11b2* expression (Figures S4B and 5Ci) and the production of aldosterone (~50 pg/mL) (Figure 5Cii and Table S1). Taken together, these data demonstrate that the *in-vitro*-produced cells respond to hormonal stimulation by producing zG and zF-specific adrenocortical steroids.

DISCUSSION

Cellular model systems are essential for studying the molecular and cellular functions of any given cell type. In the past, *in vitro* systems for studying adrenocortical cells have been limited to primary cells, which can only be maintained in culture for short periods and cell lines mainly derived from patients with cancer (Nanba et al., 2021). More recently, directed differentiation of human pluripotent cells into adrenocortical cells that secrete the

zR-specific hormone DHEA has been reported (Sakata et al., 2022). However, these cells lacked mineralocorticoid and glucocorticoid production, thus limiting their use for studying zG and zF biology. To overcome this limitation, Ruiz-Babot et al. (2023) developed a protocol that combines *in vitro* differentiation of hiPSCs with forced expression of NR5A1. Such engineered cells responded to ACTH by producing glucocorticoids in a dose-dependent manner. A potential responsiveness to stimulation with angiotensin II was not reported in this paper. Here, we report a protocol that allows the differentiation of mESCs into adrenocortical-like cells that express adrenal-specific markers, produce steroidogenic enzymes, and secrete the main mouse corticosteroids. The relatively simple protocol appears to be robust, and we have achieved differentiation with different ESC lines (*R129*, *Nr5a1-eGFP*, *C57BL/6*-not shown) in two different institutes, although some adjustments to the concentrations of the GSK3-α/β inhibitor Chiron are required to optimize mesendoderm production and cell survival for different cell lines.

Our protocol follows the major steps of embryonic differentiation and employs growth factors and signaling pathways that have been used previously for mesoderm induction. However, cellular differentiation is not only driven by diffusible signaling molecules but is also influenced by the ECM (Walma and Yamada, 2020; Knarston et al., 2020). By analyzing the data from our previously published single-cell atlas (Neirijnck et al., 2023), we discovered the presence of several ECM proteins expressed during adrenal specification, including TNC and FN1. The expression of FN1 in the developing adrenal cortex has been reported previously (Chamoux et al., 2001, 2002; Otis et al., 2007). The immunostaining in mouse embryos presented here confirmed that TNC expression is highly specific to the adrenal, but not gonadal, lineage at this developmental stage. Previous studies have shown that FN1 and TNC interact with each other (Chung et al., 1995; Lightner and Erickson, 1990; van Obberghen-Schilling et al., 2011) to provide an invasive environment for cancer cells (Ramos et al., 1998), and it is tempting to speculate that the interaction between these molecules may play a similar role in supporting differentiation and the migration of adrenal progenitors from the coelomic epithelium to a more medial position. Interestingly, culturing cells in 2D on FN1 increased NR5A1 expression. TNC exists in many different isoforms that appear to have different functions (Chiquet-Ehrismann and Chiquet, 2003; Jones and Jones, 2000). It will be interesting to conduct further studies to determine which variants are produced and how they influence the development and maturation of the adrenal cortex. Of note, our 3D aggregates express TNC and FN1 suggesting that the culture conditions recapitulate *in vivo* development.

In vitro differentiation of pluripotent stem cells rarely produces pure cell populations, but rather results in diverse cell types that often reflect various degrees of differentiation. We observed a similar diversity of cells in our 3D culture system with differentiated cells characterized by high levels of NR5A1, CYP11A1, and CYP21A1 embedded in cells expressing GATA4, a marker of the AGP (Hu et al., 2013), in addition to CITED2 and *Gli1*, two progenitor markers of the adrenal gland (Val et al., 2007). Further optimization of culture conditions may allow long-term cultures of these aggregates, as well as a full conversion of progenitors into steroid-producing cells.

Adrenals and gonads have long been thought to derive from a common primordium characterized by the expression of NR5A1 (Hatano et al., 1996). Recent single-cell sequencing studies from our lab and others have challenged this model and suggest that adrenals and gonads are specified independently, with the adrenal primordium arising in a more anterior position (Cheng et al., 2022; Neirijnck et al., 2023). The expression of the anterior markers *Gata3* and *Hoxa7* and the lack of strong induction of the posterior markers *Hoxd9* and *Hoxd11* at day 8 of differentiation suggest that our protocol does indeed target the anterior part of the urogenital ridge. In this context, it seems surprising that we detected *Cyp17a1* (data not shown), an enzyme that is important for the production of DHEA, 17-hydroxyprogesterone, or androstenedione and that is absent from adult mouse adrenals. However, a previous study reported *Cyp17a1* to be briefly expressed during mouse fetal adrenal development (E12.5–16.5) (Keeney et al., 1995). This may also explain the presence of very low levels of androstenedione in some of our samples. The absence of gonadal markers (*Foxl2*, *Sox9*, and *Hsd17b3*) and gonadal hormones and the presence of *Cyp21a1* confirm the specificity of adrenocortical differentiation.

Mineralocorticoids and glucocorticoids are produced by distinct zones of the mouse adrenal cortex. In our system, we detected primarily corticosterone, 11-dehydrocorticosterone, and 11-deoxycorticosterone suggesting that cells have adopted a zF-like differentiation status. Glucocorticoid production is tightly controlled by the hypothalamic-pituitary-adrenal axis, which induces PKA signaling in zF cells, and previous research has shown that zF differentiation is also dependent on cAMP activation (Drelon et al., 2016). It is therefore not surprising that the addition of 8-Br-cAMP in the final steps of our protocol results in cells that produce glucocorticoids rather than mineralocorticoids. Interestingly, addition of angiotensin II at day 12 of the protocol activated *Cyp11b2* and resulted in aldosterone production indicating that the cells have the capacity to also differentiate into zG cells. Altering culture conditions, perhaps by adding β-catenin activators

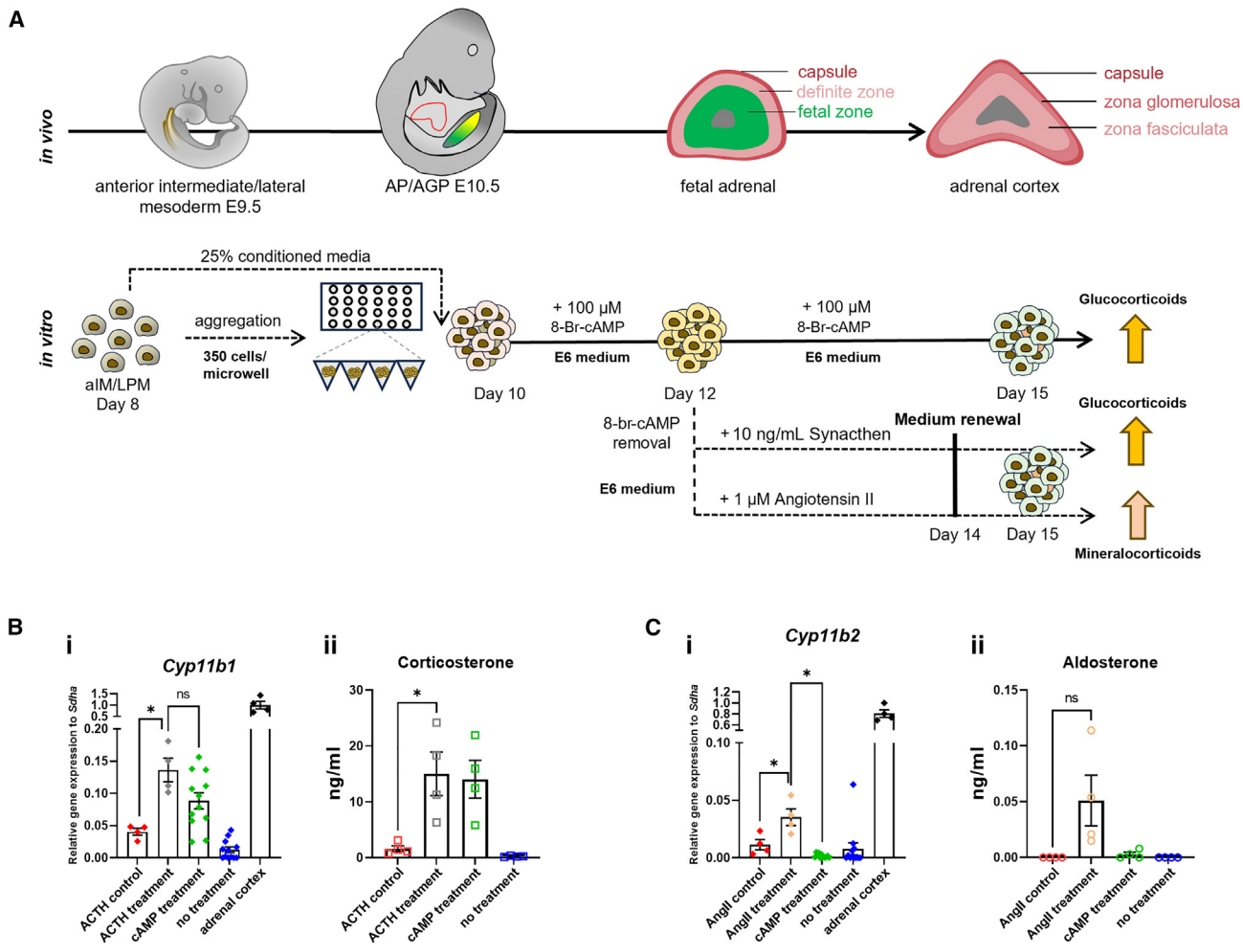

Figure 5. *In-vitro*-differentiated aggregates respond to physiological stimuli

(A) Schematic overview of adrenal cortex development *in vivo* (top panel) and stepwise overview of aggregate formation *in vitro* (bottom panel). Cells are aggregated on microwell plates and treated for 2 days with M.CM and for 2 days with 8-Br-cAMP. At day 12, 8-Br-cAMP was replaced by either Synacthen or angiotensin II for 3 days (see also experimental procedures).

(B) Analysis of ACTH (Synacthen) stimulation through *Cyp11b1* expression (i) and corticosterone production (LC-MS/MS, ii) ($n = 4$).

(C) Analysis of angiotensin II (AngII) stimulation through *Cyp11b2* expression (i) and aldosterone production (ii, LC-MS/MS) ($n = 4$). Relative mRNA expression, presented as mean ± SEM values of biological replicates (control treatment [red] $n = 4$, ACTH treatment [gray] $n = 4$, AngII treatment [beige] $n = 4$, no treatment [blue] $n = 12$, cAMP treatment [green] $n = 12$), and normalized to adult adrenal cortex + capsule (black) ($n = 4$). All statistical analysis was performed using two-tailed unpaired Welch's t test. ns, not significant; * = $p < 0.05$. See also Figure S4 and Table S1.

such as R-spondins and WNT4, which have been reported to drive zG differentiation (Heikkila et al., 2002; Vidal et al., 2016), may help to further improve mineralocorticoid production.

Given the sexually dimorphic nature of the adrenal gland (Lyraki and Schedl, 2021), it will be interesting to test the impact of sex hormones on growth and differentiation of our aggregates. In this context, it is worth noting that our culture medium contains phenol red, which has been suggested to act as a weak estrogen (Berthois et al., 1986). However, as simultaneous deletion of the estrogen receptors ERα and ERβ does not appear to impact adrenal cortex development (Couse et al., 1999), we believe an effect of this compound on our differentiation to be unlikely.

In summary, we report here the generation of functional adrenocortical steroidogenic cells from mESCs *in vitro*. We envisage that this system will become a powerful tool to study normal and abnormal development including the impact of mutations on adrenal cortex biology. Given the differences between mouse and human adrenals, a focus of

future research will be to adapt the protocol to hiPSCs. While certain differences in marker gene expression have been reported (Cheng et al., 2022), our own analysis suggests that adrenal progenitor specification at the anterior end of the urogenital ridge is highly similar between mouse and human (Neirijnck et al., 2023) and we expect the main signaling pathways to be conserved. In the long run, hiPSC-derived adrenocortical cells may pave the way for the development of cell replacement therapies for patients suffering from adrenal insufficiency or congenital adrenal hyperplasia.

EXPERIMENTAL PROCEDURES

For additional information, see supplemental experimental procedures.

Resource availability

Lead contact

Further information and requests for resources and reagents should be directed to and will be fulfilled by the corresponding authors.

Materials availability

All unique/stable reagents generated in this study are available from the lead contact.

Data and code availability

Single-cell RNA-seq data have been previously published (Neirijnck et al., 2023) and are available at the NCBI Gene Expression Omnibus database (GEO: GSE156176).

Single-cell transcriptomic analysis

Single-cell gene expression data have been computed from the previously published atlas of mouse adrenogonadal development (Neirijnck et al., 2023) using Seurat2.3.4 (Butler et al., 2018) on the entire dataset (72,273 cells) or only on mesodermal derivatives (59,619 cells) as indicated in the legend of the figures.

Animals

All animal work was conducted according to national and international guidelines and approved by the Direction Générale de la Santé of the Canton de Genève (experimentation ID GE/57/18), the French Ministry of Agriculture, and the ethical and research board of the Landesdirektion Sachsen (experimentation ID TVvG 10/2022). For paraffin embedding of embryos, the *Nr5a1-eGFP*^{Tg} mouse strain (Stallings et al., 2002) maintained on a CD1 genetic background was used. E10.5 (8 ± 2 tail somites) embryos from timed matings (day of vaginal plug = 0.5) were collected and processed for paraffin embedding. For RNA preparation, the C57BL/6J-6N strains were used. Urogenital ridges from E9.5 embryos (22 ± 2 somites), adrenal glands from E14.5 embryos, and adrenal cortex + capsule (Friedrich et al., 2021) from 12- to 14-week-old mice were collected and snap frozen until use.

mESC maintenance

Male R1 mESCs (Nagy et al., 1993) (ATCC SCRC-1011) and female *Nr5a1-eGFP* mESCs were used in this study. *Nr5a1-eGFP* mESC line was derived from *Nr5a1-eGFP*^{Tg} blastocysts, as previously described (Bryja et al., 2006). Sexing was performed by PCR with a modified protocol from McFarlane et al., (2013). mESCs were cultured in feeder-free conditions on tissue-culture treated 6-well plates (Falcon) coated with 0.1% gelatin (Sigma-Aldrich) in KnockOut DMEM (Gibco) supplemented with 15% KnockOut serum replacement (Gibco), GlutaMAX (Gibco), non-essential amino acids (Gibco), 50 μM 2-Mercaptoethanol (Gibco), 1,000 U/mL ESGRO recombinant mouse LIF protein (Sigma-Aldrich), 2 μM PD0325901 (Selleckchem), and 3 μM CHIR99021 (Sigma-Aldrich) (Tamm et al., 2013), at 37°C with 5% CO_2. Cells were passaged using 0.25% Trypsin-EDTA solution (Gibco) and Newborn Calf Serum (Gibco).

Differentiation of mESCs to aIM/LPM cells

Before differentiation, cells were kept in culture and passaged at least once. mESCs were dissociated as mentioned before and seeded at 1.8*10^4 cells/cm^2 density on new 24-well tissue culture plates (Falcon) coated with 1% Geltrex in DMEM-F12 (Gibco) at 37°C for 3–4 h. For EpiSCs differentiation, cells were cultured from day 0 to day 2 in 1:1 ReproFF2 (REPROCELL) or StemFit Basic04CT (REPROCELL):maintenance media (see the previous section) without LIF, PD0325901, and CHIR9902, and supplemented with 10 ng/mL recombinant Activin A (STEMCELL Technologies) and 10 ng/mL recombinant FGF2 (PeproTech). ReproFF2 or StemFit media resulted in comparable gene induction (data on request). For PS differentiation, cells were cultured from day 2 to day 4 in advanced RPMI 1640 (A-RPMI) (Gibco) supplemented with GlutaMAX and 7.5 μM CHIR99021. For aIM/LPM differentiation, cells were washed with A-RPMI and cultured from day 4 to day 8 in A-RPMI supplemented with 1 μM RA (Sigma-Aldrich) and 100 ng/mL FGF2. All differentiation procedures were performed at 37°C with 5% CO_2. Media were refreshed every day keeping ∼10% of initial media in the well.

Plating and differentiation on fibronectin

Wells of a 24 flat and clear bottom plate (ibidi) were coated with 1 μg/mL FN1 (Corning) in DPBS, centrifuged at ∼600 g for 2 min, incubated overnight at 4°C and brought to 37°C for an hour before plating the cells. The mesodermal conditioned medium (M.CM) from day 8 was first gathered and filtrated. Cells were dissociated using 1:1 Trypsin:DPBS and FBS (Gibco) and seeded at a 20–27*10^4 cells/cm^2 density on the FN1-coated wells. Cells were cultured from day 8 to day 10 in A-RPMI supplemented with 25% M.CM and from day 10 to day 15 in A-RPMI supplemented with 100 μM 8-Br-cAMP (Tocris). Media were refreshed at day 12 keeping ∼20% of the initial medium in the well.

Aggregate formation and differentiation

Aggregates were formed in either ultra-low attachment (ULA) plates (Corning) or in microwells (Sphericalplate 5D [Kugelmeiers] or AggreWell 400 [STEMCELL Technologies]). M.CM was harvested and cells were dissociated as described earlier. 2*10^4, 3*10^5, and 4.2*10^5 cells were seeded per well of ULA, Sphericalplate 5D, and AggreWell 400 plates, respectively. For ULA plates, aggregation was achieved by centrifugation for 2 min at ∼145 g. In microwell plates, aggregates formed spontaneously. Aggregates were cultured

from day 8 to day 10 in A-RPMI or TeSR-E6 (STEMCELL Technologies) medium supplemented with 25% M.CM. At day 10 of differentiation, an equal volume of media (A-RPMI or TeSR-E6) supplemented with 200 μM 8-Br-cAMP was added, to reach a final concentration of 100 μM 8-Br-cAMP. At day 12 of differentiation, the medium was refreshed with new media supplemented with 100 μM 8-Br-cAMP until day 15.

To respond to physiological stimuli, we removed 8-Br-cAMP from the media. We observed that 8-Br-cAMP remained very stable under our *in vitro* conditions, stimulating the cells even after 5 days. Therefore, on day 12, we replaced 2/3 of the media with an equal volume of E6 medium. This process was repeated three times. Subsequently, the aggregates were treated for 3 days with either 10 ng/mL Synacthen (Alfasigma) or 1 μM angiotensin II (Sigma-Aldrich), with a refreshment of the treatment on day 14. Control samples underwent the same media replacement and treatment schedule as the treated samples.

Steroid analysis

The amount of corticosterone released in the supernatants of the aggregates was measured by ELISA assay using the Corticosterone rat/mouse ELISA kit (Demeditec) according to the manufacturer's protocol. Optical density values were determined using a Multiskan FC Microplate Photometer (Thermo Scientific).

Furthermore, steroid profiling in cell culture supernatants was performed by LC-MS/MS as previously described (Peitzsch et al., 2015).

Statistics

Statistical tests were performed using GraphPad Prism 9 (Dotmatics). Unpaired two-tailed Welch's t test and one-way ANOVA with Welch's correction were used as indicated. Each biological replicate (i.e., independent differentiation experiment from different mESC stocks) has been run in technical replicate (2 culture wells per condition). For each biological replicate, gene expression levels and steroid amounts are expressed as the mean of the technical replicates. The number of biological replicates and statistical tests are described in the figure legends. All data are presented as the mean ± SEM. p values of <0.05 were considered statistically significant.

SUPPLEMENTAL INFORMATION

Supplemental information can be found online at https://doi.org/10.1016/j.stemcr.2024.07.010.

ACKNOWLEDGMENTS

We thank Uta Lehnert, Linda Friedrich, and Françoise Kühne for technical assistance. The authors greatly acknowledge the teams of the Platform of Resources in Imaging and Scientific Microscopy (PRISM, Institut de Biologie Valrose, University of Nice Côte d'Azur), the Core Facility Cellular Imaging (CFCI, TU Dresden), and the Animal Facility (Faculty of Medicine, University of Geneva), as well as Pauline Sararols for bioinformatic analysis. This work was supported by the Deutsche Forschungsgemeinschaft (DFG, German Research Foundation) project no. 314061271, TRR 205/2: "The Adrenal: Central Relay in Health and Disease," the Fondation pour la Recherche Médicale (grant number ARF201909009270 to Y.N.), the French National Cancer Institute and Canceropole Sud to Y.N., the Fondation ARC pour la Recherche sur le Cancer (grant number ARCPJA2023070006795 to Y.N.), La Ligue Contre le Cancer (Equipe Labelisée to A.S.), IFCAH (2022), and the ANR (ANR-11-LABX-0028-01 and ANR-18-CE14-0012 to A.S.).

AUTHOR CONTRIBUTIONS

Conceptualization, I.O., Y.N., and A.S.; methodology, I.O., Y.N., M.T., F.J.M., and M.P.; formal analysis and investigation, I.O., Y.N., and M.T.; data curation, I.O. and Y.N.; writing – original draft, I.O., Y.N., C.S., and A.S.; writing – review and editing, I.O., Y.N., C.S., and A.S.; supervision, S.N., A.S., and C.S.; funding acquisition, Y.N., S.R.B., S.N., C.S., and A.S.

DECLARATION OF INTERESTS

The authors declare no competing interests.

Received: November 23, 2023
Revised: July 25, 2024
Accepted: July 27, 2024
Published: August 22, 2024

REFERENCES

Berthois, Y., Katzenellenbogen, J.A., and Katzenellenbogen, B.S. (1986). Phenol red in tissue culture media is a weak estrogen: Implications concerning the study of estrogen-responsive cells in culture. Proc. Natl. Acad. Sci. USA *83*, 2496–2500. https://doi.org/10.1073/pnas.83.8.2496.

Bryja, V., Bonilla, S., and Arenas, E. (2006). Derivation of mouse embryonic stem cells. Nat. Protoc. *1*, 2082–2087. https://doi.org/10.1038/nprot.2006.355.

Butler, A., Hoffman, P., Smibert, P., Papalexi, E., and Satija, R. (2018). Integrating single-cell transcriptomic data across different conditions, technologies, and species. Nat. Biotechnol. *36*, 411–420. https://doi.org/10.1038/nbt.4096.

Caneparo, C., Baratange, C., Chabaud, S., and Bolduc, S. (2020). Conditioned medium produced by fibroblasts cultured in low oxygen pressure allows the formation of highly structured capillary-like networks in fibrin gels. Sci. Rep. *10*, 9291. https://doi.org/10.1038/s41598-020-66145-z.

Chamoux, E., Bolduc, L., Lehoux, J.G., and Gallo-Payet, N. (2001). Identification of extracellular matrix components and their integrin receptors in the human fetal adrenal gland. J. Clin. Endocrinol. Metab. *86*, 2090–2098. https://doi.org/10.1210/jc.86.5.2090.

Chamoux, E., Narcy, A., Lehoux, J.G., and Gallo-Payet, N. (2002). Fibronectin, laminin, and collagen IV as modulators of cell behavior during adrenal gland development in the human fetus. J. Clin. Endocrinol. Metab. *87*, 1819–1828. https://doi.org/10.1210/jcem.87.4.8359.

Cheng, K., Seita, Y., Moriwaki, T., Noshiro, K., Sakata, Y., Hwang, Y.S., Torigoe, T., Saitou, M., Tsuchiya, H., Iwatani, C., et al. (2022). The developmental origin and the specification of the

adrenal cortex in humans and cynomolgus monkeys. Sci. Adv. *8*, eabn8485. https://doi.org/10.1126/sciadv.abn8485.

Chiquet-Ehrismann, R., and Chiquet, M. (2003). Tenascins: Regulation and putative functions during pathological stress. J. Pathol. *200*, 488–499. https://doi.org/10.1002/path.1415.

Chung, C.Y., Zardi, L., and Erickson, H.P. (1995). Binding of Tenascin-C to Soluble Fibronectin and Matrix Fibrils. J. Biol. Chem. *270*, 29012–29017. https://doi.org/10.1074/jbc.270.48.29012.

Clipsham, R., Niakan, K., and McCabe, E.R. (2004). Nr0b1 and its network partners are expressed early in murine embryos prior to steroidogenic axis organogenesis. Gene Expr. Patterns *4*, 3–14. https://doi.org/10.1016/j.modgep.2003.08.004.

Couse, J.F., Hewitt, S.C., Bunch, D.O., Sar, M., Walker, V.R., Davis, B.J., and Korach, K.S. (1999). Postnatal sex reversal of the ovaries in mice lacking estrogen receptors alpha and beta. Science *286*, 2328–2331. https://doi.org/10.1126/science.286.5448.2328.

Crawford, P.A., Sadovsky, Y., and Milbrandt, J. (1997). Nuclear receptor steroidogenic factor 1 directs embryonic stem cells toward the steroidogenic lineage. Mol. Cell Biol. *17*, 3997–4006. https://doi.org/10.1128/mcb.17.7.3997.

Dedhia, P.H., Sivakumar, H., Rodriguez, M.A., Nairon, K.G., Zent, J.M., Zheng, X., Jones, K., Popova, L.V., Leight, J.L., and Skardal, A. (2023). A 3D adrenocortical carcinoma tumor platform for preclinical modeling of drug response and matrix metalloproteinase activity. Sci. Rep. *13*, 15508–15512. https://doi.org/10.1038/s41598-023-42659-0.

Drelon, C., Berthon, A., Sahut-Barnola, I., Mathieu, M., Dumontet, T., Rodriguez, S., Batisse-Lignier, M., Tabbal, H., Tauveron, I., Lefrançois-Martinez, A.M., et al. (2016). PKA inhibits WNT signalling in adrenal cortex zonation and prevents malignant tumour development. Nat. Commun. *7*, 12751. https://doi.org/10.1038/ncomms12751.

Friedrich, L., Schuster, M., Rubin de Celis, M.F., Berger, I., Bornstein, S.R., and Steenblock, C. (2021). Isolation and *in vitro* cultivation of adrenal cells from mice. STAR Protoc. *2*, 100999. https://doi.org/10.1016/j.xpro.2021.100999.

Häfner, R., Bohnenpoll, T., Rudat, C., Schultheiss, T.M., and Kispert, A. (2015). Fgfr2 is required for the expansion of the early adrenocortical primordium. Mol. Cell. Endocrinol. *413*, 168–177. https://doi.org/10.1016/j.mce.2015.06.022.

Hatano, O., Takakusu, A., Nomura, M., and Morohashi, K. (1996). Identical origin of adrenal cortex and gonad revealed by expression profiles of Ad4BP/SF-1. Gene Cell. *1*, 663–671. https://doi.org/10.1046/j.1365-2443.1996.00254.x.

Heikkila, M., Vuolteenaho, O., and Vainio, S. (2002). Wnt-4 Deficiency Alters Mouse Adrenal Cortex Function. Endocrinology *143*, 4358–4365. https://doi.org/10.1210/en.2002-220275.

Hellesen, A., Bratland, E., and Husebye, E.S. (2018). Autoimmune Addison's disease – An update on pathogenesis. Ann. Endocrinol. *79*, 157–163. https://doi.org/10.1016/j.ando.2018.03.008.

Hu, Y.C., Okumura, L.M., and Page, D.C. (2013). Gata4 Is Required for Formation of the Genital Ridge in Mice. PLoS Genet. *9*, e1003629. https://doi.org/10.1371/journal.pgen.1003629.

Ikeda, Y., Shen, W.H., Ingraham, H.A., and Parker, K.L. (1994). Developmental expression of mouse steroidogenic factor-1, an essential regulator of the steroid hydroxylases. Mol. Endocrinol. *8*, 654–662. https://doi.org/10.1210/mend.8.5.8058073.

Jones, F.S., and Jones, P.L. (2000). The tenascin family of ECM glycoproteins: Structure, function, and regulation during embryonic development and tissue remodeling. Dev. Dynam. *218*, 235–259. https://doi.org/10.1002/(SICI)1097-0177(200006)218:2<235::AID-DVDY2>3.0.CO;2-G.

Kapałczyńska, M., Kolenda, T., Przybyła, W., Zajączkowska, M., Teresiak, A., Filas, V., Ibbs, M., Bliźniak, R., Łuczewski, Ł., and Lamperska, K. (2018). 2D and 3D cell cultures – a comparison of different types of cancer cell cultures. Arch. Med. Sci. *14*, 910–919. https://doi.org/10.5114/aoms.2016.63743.

Keeney, D.S., Jenkins, C.M., and Waterman, M.R. (1995). Developmentally regulated expression of adrenal 17 alpha-hydroxylase cytochrome P450 in the mouse embryo. Endocrinology *136*, 4872–4879. https://doi.org/10.1210/endo.136.11.7588219.

King, P., Paul, A., and Laufer, E. (2009). Shh signaling regulates adrenocortical development and identifies progenitors of steroidogenic lineages. Proc. Natl. Acad. Sci. USA *106*, 21185–21190. https://doi.org/10.1073/pnas.0909471106.

Knarston, I.M., Pachernegg, S., Robevska, G., Ghobrial, I., Er, P.X., Georges, E., Takasato, M., Combes, A.N., Jørgensen, A., Little, M.H., et al. (2020). An In Vitro Differentiation Protocol for Human Embryonic Bipotential Gonad and Testis Cell Development. Stem Cell Rep. *15*, 1377–1391. https://doi.org/10.1016/j.stemcr.2020.10.009.

Kobayashi, A., Kwan, K.M., Carroll, T.J., McMahon, A.P., Mendelsohn, C.L., and Behringer, R.R. (2005). Distinct and sequential tissue-specific activitites of the LIM-class homeobox gene Lim1 for tubular morphogenesis during kidney development. Development *132*, 2809–2823. https://doi.org/10.1242/dev.01858.

Kulcenty, K., Holysz, M., and Trzeciak, W.H. (2015). SF-1 (NR5A1) expression is stimulated by the PKA pathway and is essential for the PKA-induced activation of LIPE expression in Y-1 cells. Mol. Cell. Biochem. *408*, 139–145. https://doi.org/10.1007/s11010-015-2489-9.

Labrie, F., Luu-The, V., Lin, S.X., Simard, J., and Labrie, C. (2000). Role of 17β-hydroxysteroid dehydrogenases in sex steroid formation in peripheral intracrine tissues. Trends Endocrinol. Metabol. *11*, 421–427. https://doi.org/10.1016/S1043-2760(00)00342-8.

Lam, A.Q., Freedman, B.S., Morizane, R., Lerou, P.H., Valerius, M.T., and Bonventre, J.V. (2014). Rapid and efficient differentiation of human pluripotent stem cells into intermediate mesoderm that forms tubules expressing kidney proximal tubular markers. J. Am. Soc. Nephrol. *25*, 1211–1225. https://doi.org/10.1681/ASN.2013080831.

Lightman, S.L., Birnie, M.T., and Conway-Campbell, B.L. (2020). Dynamics of ACTH and Cortisol Secretion and Implications for Disease. Endocr. Rev. *41*. bnaa002–490. https://doi.org/10.1210/endrev/bnaa002.

Lightner, V.A., and Erickson, H.P. (1990). Binding of hexabrachion (tenascin) to the extracellular matrix and substratum and its effect

on cell adhesion. J. Cell Sci. *95*, 263–277. https://doi.org/10.1242/jcs.95.2.263.

Lyraki, R., and Schedl, A. (2021). The sexually dimorphic adrenal cortex: Implications for adrenal disease. Int. J. Mol. Sci. *22*, 4889. https://doi.org/10.3390/ijms22094889.

Mahlapuu, M., Ormestad, M., Enerbäck, S., and Carlsson, P. (2001). The forkhead transcription factor Foxf1 is required for differentiation of extra-embryonic and lateral plate mesoderm. Development *128*, 155–166. https://doi.org/10.1242/dev.128.2.155.

McFarlane, L., Truong, V., Palmer, J.S., and Wilhelm, D. (2013). Novel PCR assay for determining the genetic sex of mice. Sex. Dev. *7*, 207–211. https://doi.org/10.1159/000348677.

Mugford, J.W., Sipilä, P., McMahon, J.A., and McMahon, A.P. (2008). Osr1 expression demarcates a multi-potent population of intermediate mesoderm that undergoes progressive restriction to an Osr1-dependent nephron progenitor compartment within the mammalian kidney. Dev. Biol. *324*, 88–98. https://doi.org/10.1016/j.ydbio.2008.09.010.

Nagy, A., Rossant, J., Nagy, R., Abramow-Newerly, W., and Roder, J.C. (1993). Derivation of completely cell culture-derived mice from early-passage embryonic stem cells. Proc. Natl. Acad. Sci. USA *90*, 8424–8428. https://doi.org/10.1073/pnas.90.18.8424.

Nanba, K., Blinder, A.R., and Rainey, W.E. (2021). Primary Cultures and Cell Lines for In Vitro Modeling of the Human Adrenal Cortex. Tohoku J. Exp. Med. *253*, 217–232. https://doi.org/10.1620/tjem.253.217.

Neirijnck, Y., Sararols, P., Kühne, F., Mayère, C., Weerasinghe Arachchige, L.C., Regard, V., Nef, S., and Schedl, A. (2023). Single-cell transcriptomic profiling redefines the origin and specification of early adrenogonadal progenitors. Cell Rep. *42*, 112191. https://doi.org/10.1016/j.celrep.2023.112191.

van Obberghen-Schilling, E., Tucker, R.P., Saupe, F., Gasser, I., Cseh, B., and Orend, G. (2011). Fibronectin and tenascin-C: Accomplices in vascular morphogenesis during development and tumor growth. Int. J. Dev. Biol. *55*, 511–525. https://doi.org/10.1387/ijdb.103243eo.

Otis, M., Campbell, S., Payet, M.D., and Gallo-Payet, N. (2007). Expression of extracellular matrix proteins and integrins in rat adrenal gland: Importance for ACTH-associated functions. J. Endocrinol. *193*, 331–347. https://doi.org/10.1677/JOE-07-0055.

Parker, K.L., and Schimmer, B.P. (1997). Steroidogenic Factor 1: A Key Determinant of Endocrine Development and Function.

Peitzsch, M., Dekkers, T., Haase, M., Sweep, F.C.G.J., Quack, I., Antoch, G., Siegert, G., Lenders, J.W.M., Deinum, J., Willenberg, H.S., and Eisenhofer, G. (2015). An LC-MS/MS method for steroid profiling during adrenal venous sampling for investigation of primary aldosteronism. J. Steroid Biochem. Mol. Biol. *145*, 75–84. https://doi.org/10.1016/j.jsbmb.2014.10.006.

Plachov, D., Chowdhury, K., Walther, C., Simon, D., Guenet, J.L., and Gruss, P. (1990). Pax8, a murine paired box gene expressed in the developing excretory system and thyroid gland. Development *110*, 643–651. https://doi.org/10.1242/dev.110.2.643.

Ramos, D.M., Chen, B., Regezi, J., Zardi, L., and Pytela, R. (1998). Tenascin-C matrix assembly in oral squamous cell carcinoma. Int. J. Cancer *75*, 680–687. https://doi.org/10.1002/(SICI)1097-0215(19980302)75:5<680::AID-IJC4>3.0.CO;2-V.

Ruiz-Babot, G., Balyura, M., Hadjidemetriou, I., Ajodha, S.J., Taylor, D.R., Ghataore, L., Taylor, N.F., Schubert, U., Ziegler, C.G., Storr, H.L., et al. (2018). Modeling Congenital Adrenal Hyperplasia and Testing Interventions for Adrenal Insufficiency Using Donor-Specific Reprogrammed Cells. Cell Rep. *22*, 1236–1249. https://doi.org/10.1016/j.celrep.2018.01.003.

Ruiz-Babot, G., Eceiza, A., Abollo-Jiménez, F., Malyukov, M., Carlone, D.L., Borges, K., Da Costa, A.R., Qarin, S., Matsumoto, T., Morizane, R., et al. (2023). Generation of glucocorticoid-producing cells derived from human pluripotent stem cells. Cell Rep. Methods *3*. https://doi.org/10.1016/j.crmeth.2023.100627.

Sakata, Y., Cheng, K., Mayama, M., Seita, Y., Detlefsen, A.J., Mesaros, C.A., Penning, T.M., Shishikura, K., Yang, W., Auchus, R.J., et al. (2022). Reconstitution of human adrenocortical specification and steroidogenesis using induced pluripotent stem cells. Dev. Cell *57*, 2566–2583.e8. https://doi.org/10.1016/j.devcel.2022.10.010.

Sasaki, K., Oguchi, A., Cheng, K., Murakawa, Y., Okamoto, I., Ohta, H., Yabuta, Y., Iwatani, C., Tsuchiya, H., Yamamoto, T., et al. (2021). The embryonic ontogeny of the gonadal somatic cells in mice and monkeys. Cell Rep. *35*, 109075. https://doi.org/10.1016/j.celrep.2021.109075.

Schnirman, R.E., Kuo, S.J., Kelly, R.C., and Yamaguchi, T.P. (2023). Chapter Five - The role of Wnt signaling in the development of the epiblast and axial progenitors. In Wnt Signaling in Development and Disease, T.P. Yamaguchi and D.B. Willert, eds. (Academic Press), pp. 145–180. K.B.T.-C.T. in.

Sefton, E.M., Gallardo, M., and Kardon, G. (2018). Developmental origin and morphogenesis of the diaphragm, an essential mammalian muscle. Dev. Biol. *440*, 64–73. https://doi.org/10.1016/j.ydbio.2018.04.010.

Sonoyama, T., Sone, M., Honda, K., Taura, D., Kojima, K., Inuzuka, M., Kanamoto, N., Tamura, N., and Nakao, K. (2012). Differentiation of human embryonic stem cells and human induced pluripotent stem cells into steroid-producing cells. Endocrinology *153*, 4336–4345. https://doi.org/10.1210/en.2012-1060.

Speiser, P.W., Azziz, R., Baskin, L.S., Ghizzoni, L., Hensle, T.W., Merke, D.P., Meyer-Bahlburg, H.F.L., Miller, W.L., Montori, V.M., Oberfield, S.E., et al. (2010). Congenital Adrenal Hyperplasia Due to Steroid 21-Hydroxylase Deficiency: An Endocrine Society Clinical Practice Guideline. J. Clin. Endocrinol. Metab. *95*, 4133–4160. https://doi.org/10.1210/jc.2009-2631.

Stallings, N.R., Hanley, N.A., Majdic, G., Zhao, L., Bakke, M., and Parker, K.L. (2002). Development of a transgenic green fluorescent protein lineage marker for steroidogenic factor 1. Mol. Endocrinol. *16*, 2360–2370. https://doi.org/10.1210/me.2002-0003.

Stévant, I., Kühne, F., Greenfield, A., Chaboissier, M.C., Dermitzakis, E.T., and Nef, S. (2019). Dissecting Cell Lineage Specification and Sex Fate Determination in Gonadal Somatic Cells Using Single-Cell Transcriptomics. Cell Rep. *26*, 3272–3283.e3. https://doi.org/10.1016/j.celrep.2019.02.069.

Takasato, M., Er, P.X., Chiu, H.S., Maier, B., Baillie, G.J., Ferguson, C., Parton, R.G., Wolvetang, E.J., Roost, M.S., Chuva de Sousa Lopes, S.M., and Little, M.H. (2015). Kidney organoids from

human iPS cells contain multiple lineages and model human nephrogenesis. Nature *526*, 564–568. https://doi.org/10.1038/nature15695.

Tamm, C., Galitó, S.P., and Annerén, C. (2013). A comparative study of protocols for mouse embryonic stem cell culturing. PLoS One *8*, 1–10. https://doi.org/10.1371/journal.pone.0081156.

Tosolini, M., and Jouneau, A. (2016). From Naive to Primed Pluripotency: In Vitro Conversion of Mouse Embryonic Stem Cells in Epiblast Stem Cells. In Embryonic Stem Cell Protocols, K. Turksen, ed. (Springer New York), pp. 209–216.

Val, P., Martinez-Barbera, J.P., and Swain, A. (2007). Adrenal development is initiated by Cited2 and Wt1 through modulation of Sf-1 dosage. Development *134*, 2349–2358. https://doi.org/10.1242/dev.004390.

Vidal, V., Sacco, S., Rocha, A.S., Da Silva, F., Panzolini, C., Dumontet, T., Doan, T.M.P., Shan, J., Rak-Raszewska, A., Bird, T., et al. (2016). The adrenal capsule is a signaling center controlling cell renewal and zonation through Rspo3. Genes Dev. *30*, 1389–1394. https://doi.org/10.1101/gad.277756.116.

Walczak, E.M., and Hammer, G.D. (2015). Regulation of the adrenocortical stem cell niche: Implications for disease. Nat. Rev. Endocrinol. *11*, 14–28. https://doi.org/10.1038/nrendo.2014.166.

Walma, D.A.C., and Yamada, K.M. (2020). The extracellular matrix in development. Development *147*, dev175596. https://doi.org/10.1242/dev.175596.

Wood, M.A., Acharya, A., Finco, I., Swonger, J.M., Elston, M.J., Tallquist, M.D., and Hammer, G.D. (2013). Fetal adrenal capsular cells serve as progenitor cells for steroidogenic and stromal adrenocortical cell lineages in M. musculus. Development *140*, 4522–4532. https://doi.org/10.1242/dev.092775.